Comparison of ozone profiles and influences from the tertiary ozone maximum in the night-to-day ratio above Switzerland

Lorena Moreira[1], Klemens Hocke[1], and Niklaus Kämpfer[1]

[1]Institute of Applied Physics and Oeschger Centre for Climate Change Research, University of Bern, Bern, Switzerland

Correspondence to: L. Moreira (lorena.moreira@iap.unibe.ch)

Abstract. Stratospheric and middle mesospheric ozone profiles have been continually measured by the GROMOS (GROund-based Millimeter-wave Ozone Spectrometer) microwave radiometer since 1994 above Bern, Switzerland (46.95°N, 7.44°E, 577 m). GROMOS is part of the Network for the Detection of Atmospheric Composition Change (NDACC). A new version for the retrieval of ozone profiles has been developed with the aim to improve the altitude range of retrieval profiles. GROMOS
5 profiles from this new retrieval version have been compared to coincident ozone profiles obtained by the satellite limb sounder Aura/MLS. The study covers the stratosphere and middle mesosphere from 50 to 0.05 hPa (from 21 to 70 km) and extends over the period from July 2009 to November 2016, which results in more than 3500 coincident profiles available for the comparison. GROMOS and Aura/MLS profiles agree within 3% for the altitude range from 25 to 55 km, with standard deviations of the mean relative differences around 5% from 30 to 40 km and tending to 10% towards the lower and upper stratosphere.
10 Above the stratosphere, the mean relative differences and its standard deviations are increasing with altitude up to 50% at 70 km. In addition, we have observed the annual variation of nighttime ozone in the middle mesosphere, at 0.05 hPa (70 km), characterised by the enhancement of ozone during wintertime for both ground-based and space-based measurements. This behaviour is explained by the middle mesospheric maximum of ozone (MMM). On the other hand, the amplitude of the diurnal variation, night-to-day ratio (NDR), is not as strong as the observed one at higher latitudes, nevertheless we observe the winter
15 anomaly of the night-to-day ratio.

1 Introduction

Passive millimeter wave radiometry is a well-established technique to monitor atmospheric constituents by detecting the radiation emitted by the rotational transitions of the molecules. It makes use of the spectral properties of the atmospheric species in order to derive information about its distribution in the atmosphere. The main advantages of this technique are the inde-
20 pendence of solar irradiation and its insensitivity to weather conditions and aerosols. Additionally it offers a good temporal resolution of 1 hour. Measurements of ozone performed by this technique have been indispensable in monitoring changes in the ozone layer and improving the comprehension of the processes that control ozone abundances. The ozone molecule, in spite of its small abundance in the atmosphere, plays vital roles. Stratospheric ozone plays a beneficial role by absorbing most of the biologically harmful ultraviolet sunlight. The absorption of UV radiation by ozone creates a source of heat, therefore
25 ozone plays a key role in the temperature structure of the Earth's atmosphere. Changes in the stratospheric ozone concentration

alter the radiative balance of the atmosphere, the atmospheric composition and the dynamics of the atmosphere. Thus, continuous long-term monitoring of ozone is essential for the detection of long-term trends of the stratospheric ozone layer. The ground-based ozone radiometer GROMOS (GROund-based Millimeter-wave Ozone Spectrometer) is part of the Network for the Detection of Atmospheric Composition Change (NDACC). In order to satisfy the requirements of accuracy and stability

5 the validation of instruments is necessary. There have been a number of comparisons in the past, showing that GROMOS is a reliable tool to measure stratospheric and lower mesospheric ozone (WMO, 2014; Studer et al., 2013; van Gijsel et al., 2010; Keckhut et al., 2010; Dumitru et al., 2006).

This manuscript presents a comparison between the data from the ground-based instrument GROMOS and the space-based instrument Aura/MLS for the time interval from July 2009 to November 2016 covering the stratosphere and the middle meso-

10 sphere, which corresponds to the altitude range from 20 to 70 km (50 to 0.05 hPa). Furthermore, we have performed an analysis of the diurnal variation and the amplitude of the diurnal variation (night-to-day ratio) of middle mesospheric ozone, at 0.05 hPa (70 km). The diurnal variation of ozone in the lower and middle mesosphere is observed as an increase in ozone after sunset and a decrease after sunrise. Atomic oxygen densities are comparable to, and even greater than those of ozone, so that the recombination reaction explains the daily cycle of ozone in the mesosphere (Brasseur and Solomon, 2005). Moreover, we

15 observe the annual variation of the nighttime mesospheric ozone with a maximum in wintertime and a minimum in summertime. This maximum of mesospheric ozone during nighttime in winter is related to the middle mesospheric maximum of ozone (MMM) (e.g., Sonnemann et al., 2007; Hartogh et al., 2004) also known as the tertiary ozone maximum (e.g., Sofieva et al., 2009; Degenstein et al., 2005; Marsh et al., 2001). Sonnemann et al. (2007) reported that the MMM is an effect occuring at high latitudes close to the polar night terminator around 72 km altitude during nighttime in winter and extends into middle lati-

20 tudes with decreasing amplitude. Marsh et al. (2001) interpreted the tertiary peak by considering that in the middle mesosphere during winter, with solar zenith angle close to $90°$, the atmosphere becomes optically thick to UV radiation at wavelengths below 185 nm and since photolysis of water vapour is the primary source of odd-hydrogen, reduced UV radiation results in less odd-hydrogen. The shortage of odd-hydrogen for the catalytic depletion of odd-oxygen, and there is no decrease in the production of odd-oxygen, results in an increase in odd-oxygen. This results in higher ozone concentration because atomic

25 oxygen recombination remains as a significant source of ozone in the mesosphere. Additionally, Hartogh et al. (2004) extended the interpretation by considering the very slow decrease of the ozone dissociation rate with increasing solar zenith angle.

This publication presents a new comparison between a ground-based instrument (GROMOS) and a spaced-based instrument (Aura/MLS). The next section describes briefly both instruments and measurement techniques. The results of the comparison are shown in Section 3. Section 4 analyses the night-to-day variability and provides a short discussion. And finally, the

30 conclusions are summarised in Section 5.

2 Instruments and measurement techniques

2.1 The ground-based microwave radiometer GROMOS

This study is based on stratospheric and mesospheric ozone volume mixing ratio (VMR) profiles observed by GROMOS. The ground-based millimeter wave ozone spectrometer has been operating in Bern, Switzerland (46.95°N, 7.44°E, 577 m) since November 1994 in the framework of the Network for the Detection of Atmospheric Composition Change (NDACC). The instrument measures the thermal microwave emission of the pressure broadened rotational transition of ozone at 142.175 GHz. The vertical distribution of ozone VMR can be retrieved from the measured spectral line since it contains information on the

5   altitude distribution of the emitting molecule due to the pressure broadening. The retrieval procedure is performed through the Atmospheric Radiative Transfer Simulator (ARTS2) (Eriksson et al., 2011) which is used as a forward model to simulate the atmospheric radiative transfer in a modelled atmosphere and so calculate the ozone spectrum of this modelled atmosphere. A priori information is required in the inversion process and is taken from a monthly varying climatology from ECMWF reanalysis until available (70 km) and extended by an Aura/MLS climatology (2004 to 2010) above (Studer et al., 2013). The

10   accompanying Matlab package Qpack2 (Eriksson et al., 2005) compares the modelled spectrum with the measured spectrum and derives the best estimate of the vertical profile by using the optimal estimation method (OEM) (Rodgers, 1976). The OEM also provides a characterisation and formal analysis of the uncertainties (Rodgers, 1990). We have recently developed a new retrieval version, version 150. The difference with the former version, version 2021, is that the uncertainty of the a priori is kept constant with the altitude, thus optimizing the averaging kernels and improving the measurement response in

15   the lower stratosphere. The a priori covariance matrix has a constant value for the diagonal elements of 2 ppm and for the off-diagonal elements the values decay exponentially with a correlation length of 3 km. This new retrieval version is performed with a variable error depending on the tropospheric transmission incorporated in the covariance matrix of $\Delta T_b' = 0.5 + \frac{\Delta T_b}{e^{-\tau}}$, $\Delta T_b = \frac{T_{rec}}{\sqrt{B \cdot t}}$ is given by the radiometer noise equation. In addition, a constant error of 0.5 K is considered as a systematic bias of the spectra. The inversion of the spectra is performed in case of transmission factor larger than 0.2. We have reprocessed

20   the data with hourly time resolution. Figure 1 displays an example of a GROMOS retrieval accomplished by the new retrieval version 150. The left panel show the a priori (green line) and the retrieved profile (blue line) measured in July 2013 at noon. In the middle panel are represented the averaging kernels (AVK) and the area of the averaging kernels (measurement response). The AVK are multiplied by 4 in order to be displayed along with the measurement response (red line). The AVK-lines are grey except for some selected altitudes, which are shown in different colours to make the Figure 1 easier to interpret. AVK

25   are a representation of the weighting of information content of the retrieval parameters therefore an estimate of the a priori contribution to the retrieval can be obtained by the area of the AVK (measurement response). It is considered a reliable altitude range of the retrieval when the true state dominates over the a priori information, i.e. where the measurement response is larger than 0.8 (an a priori contribution smaller than 20%). The measurement response shown in Figure 1 is around 1 from 18 to 70 km. The magenta line in the right panel shows the altitude peak of the corresponding kernels and proves that the AVK peak

30   at its nominal altitude for the considered altitude range. And finally, the cyan line displays the vertical resolution which is quantified by the full width at half maximum of the averaging kernels. The vertical resolution of this new retrieval version of

GROMOS lies from 10 to 15 km below 40 km altitude and from 15 to 20 km below 70 km altitude.

For technical details, measurement principle of the instrument, see for example Moreira et al. (2015) and Peter (1997) and references included therein.

2.2 The Aura microwave limb sounder

The Microwave Limb Sounder (MLS) is a passive microwave limb-sounding radiometer onboard the NASA Aura satellite. The Aura spacecraft was launched in 2004 into a near polar, sun-synchronous orbit with a period of approximately 100 minutes. The satellite overpasses our location (at northern mid-latitudes) twice a day, approximately around noon and midnight. The standard product for ozone is derived from MLS radiance measurements near 240 GHz. The present study has used ozone profiles from version 4.2. Details about the Aura mission can be found in Waters et al. (2006).

3 Comparison of Aura/MLS and GROMOS

The vertical resolution of the Aura/MLS is within 3.5 km in the stratosphere and up to 5.5 km in the middle mesosphere. Therefore in order to compare ozone profiles of GROMOS with Aura/MLS, an averaging kernel smoothing is applied to the ozone profiles of the satellite data. The smoothed profile of Aura/MLS adjusted to the vertical resolution of GROMOS is expressed as: $\mathbf{X}_{MLS,low} = \mathbf{X}_{a,GROMOS} + \mathbf{A}_{GROMOS} \cdot (\mathbf{X}_{MLS,high} - \mathbf{X}_{a,GROMOS})$. $\mathbf{A}_{GROMOS}$ is the averaging kernel matrix of GROMOS, $\mathbf{X}_{MLS,high}$ is the measured Aura/MLS profile and $\mathbf{X}_{a,GROMOS}$ is the a priori profile used during the retrieval procedure of GROMOS. The application of averaging kernel smoothing for the comparison of profiles with different altitude resolutions has been introduced and described by Tsou et al. (1995).

Every profile utilised in the comparison between Aura/MLS and GROMOS should be coincident in time and space. The requirement of time coincidence is satisfied when both measurements are within 1 hour in time. The selected criterion for spatial coincidence is that horizontal distances between the sounding volumes of the satellite and the ground station have to be smaller than 8° in latitude and longitude ($d <$800 km).

The present study extends over the period from July 2009 to November 2016 and covers the stratosphere and middle mesosphere from 50 to 0.05 hPa (from 21 to 70 km), and according with the compliance of the spatial and temporal criteria, more than 3500 coincident profiles are available for the comparison. The mean ozone profiles and its standard deviations of the collocated and coincident measurements of both instruments are shown in the right panel of Figure 2, GROMOS–blue line and blue area and Aura/MLS–red line and red area, respectively. The relative difference profile in percent given by $(\mathbf{X}_{MLS,low} - \mathbf{X}_{GROMOS})/\mathbf{X}_{GROMOS}$ is displayed in the middle panel of Figure 2 along with the standard deviation of the differences (blue area). The green line delimits the ± 10% area. The mean relative differences between GROMOS and Aura/MLS during this time period are within 3% between 30 and 0.35 hPa (25 to 55 km) and progressively increasing to 50% at 70 km. The standard deviation of the mean relative differences are around 5% for the altitude range from 30 to 40 km and tending to roughly 10% toward the lower and upper stratosphere, and up to 50% in the middle mesosphere. The mean profile of the absolute differences is shown in the right panel of Figure 2. This result is in agreement with other comparisons performed

between ground-based microwave radiometers and spaced-based instruments above Switzerland, where the bias among data sets relied within 5–10 % in the stratosphere and up to 50% towards the mesosphere (Studer et al., 2013; Barras et al., 2009; Hocke et al., 2007; Dumitru et al., 2006; Calisesi et al., 2005).

For an overview of the coincident profiles, the ozone VMR (ppm) time series of GROMOS (blue line) and Aura/MLS (red line) are displayed in Figure 3 for different pressure levels. Short temporal fluctuations (periods < 4 days) are suppressed by a moving average over 30 data points of both time series. The agreement between both ground-based and satellite-based instruments depends upon altitude and time. A negative deviation of GROMOS series with respect to Aura/MLS occurs in the

5 lower stratosphere. On the other hand a positive deviation of GROMOS with respect to Aura/MLS is observed in the middle stratosphere for summers 2011, 2012, 2014 and 2015. Further, we notice a negative bias of GROMOS during summer 2016 from the stratopause towards the mesosphere. In Figure 4 are shown the scatter plots of GROMOS and Aura/MLS at the same pressure levels as Figure 3. An almost perfect agreement between the linear regression lines of the observations (black lines) and the identity of both data sets (O_3(Aura/MLS)=O_3(GROMOS)–green lines) is observed, except for the lower stratosphere

10 where we find the negative deviation of GROMOS with respect to Aura/MLS. The linear fit deviates from the identity where there is less ozone in the case of GROMOS during winter in the middle stratosphere as we also observe in Figure 3, along with the positive deviation of GROMOS with respect to Aura/MLS during some summers. The calculation of the correlation coefficients also reveals good agreement with $r > 0.75$ for all altitudes levels except for the altitudes above 50 km where r is around 0.55. To sum up we can reiterate the fairly good agreement obtained for the comparison between ozone VMR profiles

15 recorded by the ground-based instrument (GROMOS) and by the spaced-based instrument (Aura/MLS) during the time interval between July 2009 and November 2016 for the altitude range from 20 to 70 km.

4   Analysis of the night-to-day ratio

The diurnal variation of mesospheric ozone is characterised by an increase at the beginning of the nighttime and by a decrease after sunrise. This effect is explained by the recombination of atomic and molecular oxygen (e.g., Brasseur and Solomon,

20 2005). Because the ozone distribution in the mesosphere is mainly controlled by photochemistry, it depends strongly on the solar zenith angle (Nagahama et al., 2003), therefore an annual variation is expected in mesospheric ozone. Figure 5 shows both the diurnal variation of mesospheric ozone and the annual variation of nighttime mesospheric ozone. To analyse the variability of mesospheric ozone we have used ozone VMR measurements coincident in space and in time recorded by GROMOS and by Aura/MLS for the time period from July 2009 to November 2016. The first panel of Figure 5 displays the O_3 VMR measured

25 at noon (GROMOS in red, Aura/MLS in orange) and at midnight (GROMOS in blue, Aura/MLS in cyan) at 0.05 hPa (70 km) for the already mentioned time period. We define as midnight (noon) value the average between the values recorded within 2 hours around midnight (noon). The daytime mesospheric ozone does not show any distinct annual variation. On the other hand, the annual variation of nighttime mesospheric ozone is characterised by a maximum in wintertime and a minimum in summertime. The second panel of Figure 5 shows the evolution of the midnight mesospheric ozone throughout the year

30 averaged for the time interval from July 2009 to November 2016. A closer observation shows that the annual variation of the

nighttime ozone exhibits a primary maximum over wintertime and a secondary maximum around springtime. Our results at Bern (Switzerland, 46.95°N, 7.44°E) are in agreement with the ones observed at Lindau (Gernamy, 51.66°N, 10.13°E) by Sonnemann et al. (2007). Differences occur in the amplitudes where the maximum values of GROMOS do not exceed 1.5 ppm, 1.2 ppm in the case of Aura/MLS, whereas at Lindau the maximum values exceed 3 ppm at 70 km. This maximum of mesospheric ozone during nighttime in winter is related to the middle mesospheric maximum of ozone (MMM) (e.g., Sonnemann et al., 2007; Hartogh et al., 2004) also known as the tertiary ozone maximum (e.g., Sofieva et al., 2009; Degenstein et al., 2005; Marsh et al., 2001). During winter, the photodissociation rate of water is reduced at high latitudes which leads to a decrease of catalytic ozone depletion by odd hydrogen. Furthermore, we have analysed the amplitude of the diurnal variation, the night-to-day-ratio (NDR). The NDR is closely related to the MMM, but it is also related to the change of the diurnal variation from winter to summer (Sonnemann et al., 2007). The annual variation of the NDR is modulated by oscillations of planetary time scale (Sonnemann et al., 2007). Sofieva et al. (2009) reported that during a sudden stratospheric warming event the tertiary ozone maximum can decrease significantly or can even be completely destroyed. Hocke (2017) has shown the loss of the tertiary ozone layer in the polar mesosphere due to the solar proton event in November 2004.

The first panel of Figure 6 displays the NDR of GROMOS (blue line) and Aura/MLS (red line) at 0.05 hPa (70 km) for the time interval from July 2009 to November 2016 while the second panel shows its evolution throughout the year averaged for the time interval under assessment. The orange line (Aura/MLS) and the cyan line (GROMOS) depicted in the second panel of Figure 6 shown a moving average over 10 data points with the aim to clarify the understanding of the Figure 6. The Aura/MLS and the GROMOS series depicted in Figure 5 and Figure 6 have been smoothed in time by a moving average over 30 data points. Both the ground-based and the satellite-based instruments confirm the expected winter anomaly of the NDR, also observed at Lindau by Sonnemann et al. (2007), although with smaller amplitudes. We observe winter-to-summer values of a factor of one to two, whereas at Lindau it is shown winter-to-summer values of a factor of two to three at 70 km (Sonnemann et al., 2007). Thus, despite the definition of the MMM restricted to high latitudes we can report its observation with smaller amplitude at mid-latitudes.

5 Conclusions

Stratospheric and middle mesospheric ozone profiles for the period from July 2009 to November 2016 recorded by the ground-based instrument GROMOS and by the spaced-based instrument Aura/MLS were used to perform a comparison and to evaluate the diurnal variability and the amplitude of the diurnal variability, night-to-day ratio (NDR). The agreement between measurements coincident in space and time of both data sets is within 3% between 25 to 55 km. At upper altitudes (up to 70 km) the mean relative ozone differences are within a range of 50%. In general terms we can report a good agreement among the new retrieval version (v150) of GROMOS and the version 4.2 of Aura/MLS. Further, we observe extensions of the middle mesospheric maximum of ozone (MMM) during winter towards northern mid-latitudes. This effect is smaller in amplitude at mid-latitudes compared to high latitudes. Moreover, the winter anomaly of nighttime mesospheric ozone is observed by GROMOS and Aura/MLS above Bern.

6 Code availability

Routines for data analysis are available upon request by Lorena Moreira.

7 Data availability

The data from the GROMOS microwave radiometer is available via http://ftp.cpc.ncep.noaa.gov/ndacc/station/bern/hdf/mwave.
MLS v4.2 data are available from the NASA Goddard Space Flight Center Earth Sciences Data and Information Services Cen-
5 ter (GES DISC), http://disc.sci.gsfc.nasa.gov/Aura/data-holdings/MLS/index.shtml.

Author contributions. Klemens Hocke performed the retrieval of the GROMOS data. Lorena Moreira carried out the data analysis. Niklaus
Kämpfer is the principal investigator of the radiometry project. All authors have contributed to the interpretation of the data set.

Acknowledgements. This work was supported by the Swiss National Science Foundation under Grant 200020 - 160048 and MeteoSwiss
GAW Project: "Fundamental GAW parameters measured by microwave radiometry".

References

Barras, E. M., Ruffieux, D., and Hocke, K.: Stratospheric ozone profiles over Switzerland measured by SOMORA, ozonesonde and MLS/AURA satellite, International Journal of Remote Sensing, 30, 4033–4041, doi:10.1080/01431160902821890, http://dx.doi.org/10.1080/01431160902821890, 2009.

Brasseur, G. P. and Solomon, S.: Aeronomy of the middle atmosphere: chemistry and physics of the stratosphere and mesosphere, vol. 32 of *Atmospheric and Oceanographic Science Library*, Springer Science, 2005.

Calisesi, Y., Soebijanta, V. T., and van Oss, R.: Regridding of remote soundings: Formulation and application to ozone profile comparison, Journal of Geophysical Research: Atmospheres, 110, n/a–n/a, doi:10.1029/2005JD006122, http://dx.doi.org/10.1029/2005JD006122, d23306, 2005.

Degenstein, D. A., Gattinger, R. L., Lloyd, N. D., Bourassa, A. E., Wiensz, J. T., and Llewellyn, E. J.: Observations of an extended mesospheric tertiary ozone peak, Journal of Atmospheric and Solar-Terrestrial Physics, 67, 1395 – 1402, doi:http://dx.doi.org/10.1016/j.jastp.2005.06.019, http://www.sciencedirect.com/science/article/pii/S1364682605001410, 2005.

Dumitru, M., Hocke, K., Kämpfer, N., and Calisesi, Y.: Comparison and validation studies related to ground-based microwave observations of ozone in the stratosphere and mesosphere, Journal of Atmospheric and Solar-Terrestrial Physics, 68, 745 – 756, doi:http://dx.doi.org/10.1016/j.jastp.2005.11.001, //www.sciencedirect.com/science/article/pii/S1364682605003305, 2006.

Eriksson, P., Jiménez, C., and Buehler, S. A.: Qpack, a general tool for instrument simulation and retrieval work, Journal of Quantitative Spectroscopy and Radiative Transfer, 91, 47 – 64, doi:http://dx.doi.org/10.1016/j.jqsrt.2004.05.050, 2005.

Eriksson, P., Buehler, S., Davis, C., Emde, C., and Lemke, O.: ARTS, the atmospheric radiative transfer simulator, version 2, Journal of Quantitative Spectroscopy and Radiative Transfer, 112, 1551 – 1558, doi:http://dx.doi.org/10.1016/j.jqsrt.2011.03.001, 2011.

Hartogh, P., Jarchow, C., Sonnemann, G. R., and Grygalashvyly, M.: On the spatiotemporal behavior of ozone within the upper mesosphere/mesopause region under nearly polar night conditions, Journal of Geophysical Research: Atmospheres, 109, n/a–n/a, doi:10.1029/2004JD004576, http://dx.doi.org/10.1029/2004JD004576, 2004.

Hocke, K.: Response of the middle atmosphere to the geomagnetic storm of November 2004, Journal of Atmospheric and Solar-Terrestrial Physics, 154, 86 – 91, doi:http://dx.doi.org/10.1016/j.jastp.2016.12.013, http://www.sciencedirect.com/science/article/pii/S1364682616303613, 2017.

Hocke, K., Kämpfer, N., Ruffieux, D., Froidevaux, L., Parrish, A., Boyd, I., von Clarmann, T., Steck, T., Timofeyev, Y. M., Polyakov, A. V., and Kyrölä, E.: Comparison and synergy of stratospheric ozone measurements by satellite limb sounders and the ground-based microwave radiometer SOMORA, Atmospheric Chemistry and Physics, 7, 4117–4131, doi:10.5194/acp-7-4117-2007, http://www.atmos-chem-phys.net/7/4117/2007/, 2007.

Keckhut, P., Hauchecorne, A., Blanot, L., Hocke, K., Godin-Beekmann, S., Bertaux, J.-L., Barrot, G., Kyrölä, E., van Gijsel, J. A. E., and Pazmino, A.: Mid-latitude ozone monitoring with the GOMOS-ENVISAT experiment version 5: the noise issue, Atmospheric Chemistry and Physics, 10, 11 839–11 849, doi:10.5194/acp-10-11839-2010, http://www.atmos-chem-phys.net/10/11839/2010/, 2010.

Marsh, D., Smith, A., Brasseur, G., Kaufmann, M., and Grossmann, K.: The existence of a tertiary ozone maximum in the high-latitude middle mesosphere, Geophysical Research Letters, 28, 4531–4534, doi:10.1029/2001GL013791, http://dx.doi.org/10.1029/2001GL013791, 2001.

Moreira, L., Hocke, K., Eckert, E., von Clarmann, T., and Kämpfer, N.: Trend analysis of the 20-year time series of stratospheric ozone profiles observed by the GROMOS microwave radiometer at Bern, Atmospheric Chemistry and Physics, 15, 10 999–11 009, doi:10.5194/acp-15-10999-2015, http://www.atmos-chem-phys.net/15/10999/2015/, 2015.

5   Nagahama, T., Nakane, H., Fujinuma, Y., Ogawa, H., Mizuno, A., and Fukui, Y.: A semiannual variation of ozone in the middle mesosphere observed with the millimeter-wave radiometer at Tsukuba, Japan, Journal of Geophysical Research: Atmospheres, 108, n/a–n/a, doi:10.1029/2003JD003724, http://dx.doi.org/10.1029/2003JD003724, 4684, 2003.

Peter, R.: The ground-based millimeter-wave ozone spectrometer-GROMOS, IAP Research Report, University of Bern, Bern, Switzerland, 1997.

10 Rodgers, C. D.: Retrieval of atmospheric temperature and composition from remote measurements of thermal radiation, Reviews of Geophysics, 14, 609–624, doi:10.1029/RG014i004p00609, 1976.

Rodgers, C. D.: Characterization and error analysis of profiles retrieved from remote sounding measurements, Journal of Geophysical Research: Atmospheres, 95, 5587–5595, doi:10.1029/JD095iD05p05587, http://dx.doi.org/10.1029/JD095iD05p05587, 1990.

Sofieva, V. F., Kyrölä, E., Verronen, P. T., Seppälä, A., Tamminen, J., Marsh, D. R., Smith, A. K., Bertaux, J.-L., Hauchecorne, A.,

15   Dalaudier, F., Fussen, D., Vanhellemont, F., Fanton d'Andon, O., Barrot, G., Guirlet, M., Fehr, T., and Saavedra, L.: Spatio-temporal observations of the tertiary ozone maximum, Atmospheric Chemistry and Physics, 9, 4439–4445, doi:10.5194/acp-9-4439-2009, http://www.atmos-chem-phys.net/9/4439/2009/, 2009.

Sonnemann, G., Hartogh, P., Jarchow, C., Grygalashvyly, M., and Berger, U.: On the winter anomaly of the night-to-day ratio of ozone in the middle to upper mesosphere in middle to high latitudes, Advances in Space Research, 40, 846 – 854,

20   doi:http://dx.doi.org/10.1016/j.asr.2007.01.039, http://www.sciencedirect.com/science/article/pii/S0273117707000464, 2007.

Studer, S., Hocke, K., Pastel, M., Godin-Beekmann, S., and Kämpfer, N.: Intercomparison of stratospheric ozone profiles for the assessment of the upgraded GROMOS radiometer at Bern, Atmospheric Measurement Techniques Discussions, 6, 6097–6146, doi:10.5194/amtd-6-6097-2013, http://www.atmos-meas-tech-discuss.net/6/6097/2013/, 2013.

Tsou, J. J., Connor, B. J., Parrish, A., McDermid, I. S., and Chu, W. P.: Ground-based microwave monitoring of middle atmosphere ozone:

25   Comparison to lidar and Stratospheric and Gas Experiment II satellite observations, Journal of Geophysical Research: Atmospheres, 100, 3005–3016, doi:10.1029/94JD02947, http://dx.doi.org/10.1029/94JD02947, 1995.

van Gijsel, J. A. E., Swart, D. P. J., Baray, J.-L., Bencherif, H., Claude, H., Fehr, T., Godin-Beekmann, S., Hansen, G. H., Keckhut, P., Leblanc, T., McDermid, I. S., Meijer, Y. J., Nakane, H., Quel, E. J., Stebel, K., Steinbrecht, W., Strawbridge, K. B., Tatarov, B. I., and Wolfram, E. A.: GOMOS ozone profile validation using ground-based and balloon sonde measurements, Atmospheric Chemistry and

30   Physics, 10, 10 473–10 488, doi:10.5194/acp-10-10473-2010, http://www.atmos-chem-phys.net/10/10473/2010/, 2010.

Waters, J. W., Froidevaux, L., Harwood, R. S., Jarnot, R. F., Pickett, H. M., Read, W. G., Siegel, P. H., Cofield, R. E., Filipiak, M. J., Flower, D. A., Holden, J. R., Lau, G. K., Livesey, N. J., Manney, G. L., Pumphrey, H. C., Santee, M. L., Wu, D. L., Cuddy, D. T., Lay, R. R., Loo, M. S., Perun, V. S., Schwartz, M. J., Stek, P. C., Thurstans, R. P., Boyles, M. A., Chandra, K. M., Chavez, M. C., Chen, G.-S., Chudasama, B. V., Dodge, R., Fuller, R. A., Girard, M. A., Jiang, J. H., Jiang, Y., Knosp, B. W., LaBelle, R. C., Lam, J. C., Lee, K. A., Miller, D.,

35   Oswald, J. E., Patel, N. C., Pukala, D. M., Quintero, O., Scaff, D. M., Snyder, W. V., Tope, M. C., Wagner, P. A., and Walch, M. J.: The Earth observing system microwave limb sounder (EOS MLS) on the aura Satellite, IEEE Transactions on Geoscience and Remote Sensing, 44, 1075–1092, doi:10.1109/TGRS.2006.873771, 2006.

WMO: Scientific Assessment of Ozone Depletion: 2014, Global Ozone Research and Monitoring Project–Report No.55, 416 pp. Geneva,

270   Switzerland, 2014.
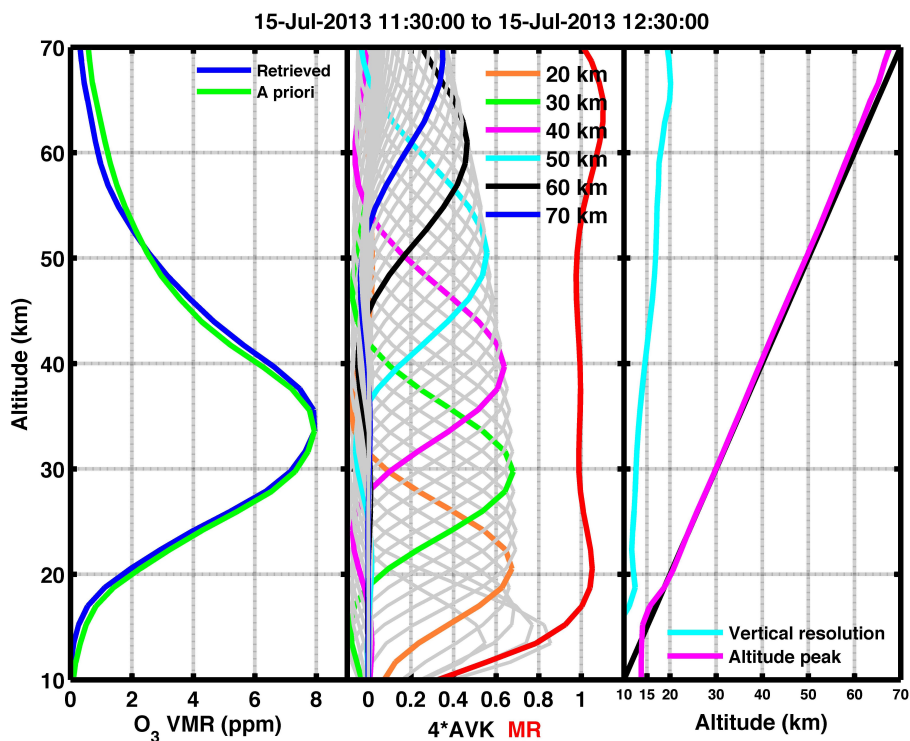
Figure 1. Example of an a priori profile and a retrieved ozone profile (green and blue lines in the left panel, respectively), averaging kernels (grey and colour lines in the middle panel), the measurement response (red line in the panel), vertical resolution (cyan line in the right panel) and altitude peak (magenta line in the right panel) of the GROMOS retrieval version 150 for July 15, 2013 with an integration time of 1 hour
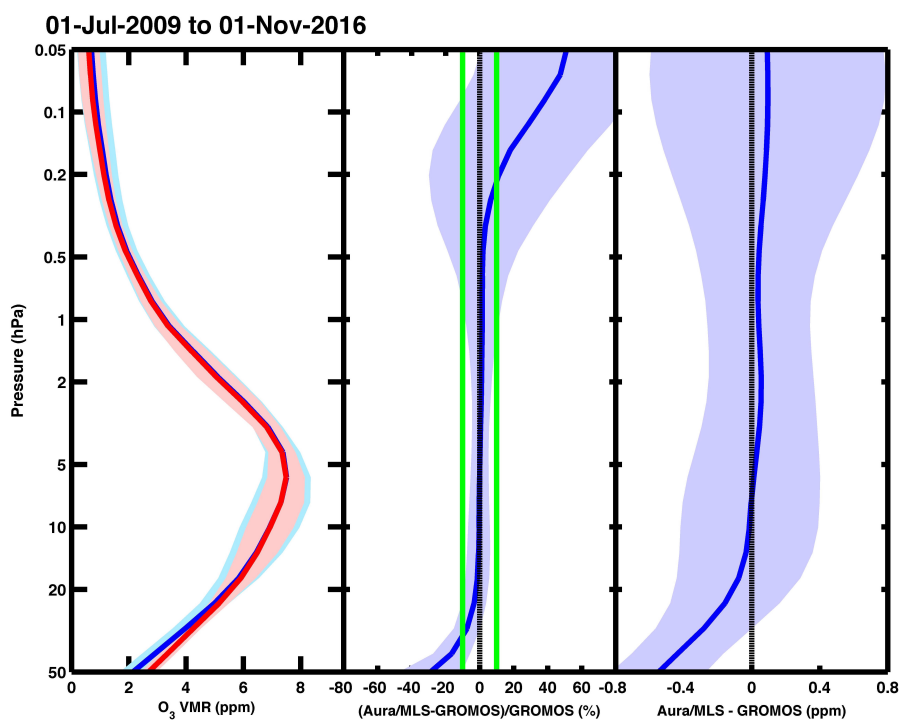
Figure 2. Mean ozone profiles recorded by GROMOS (blue line) and by Aura/MLS (red line) for the time interval between July 2009 and November 2016 are shown in the left panel. The blue area (GROMOS) and the red area (Aura/MLS) are the standard deviations of the coincident measurements. In the middle panel is represented the mean relative difference profile between data of both instruments, GROMOS as reference. The blue area represents the standard deviation of the differences. The green line delimits the ± 10% area. The mean absolute difference profile and its uncertainty (blue area) is displayed in the right panel
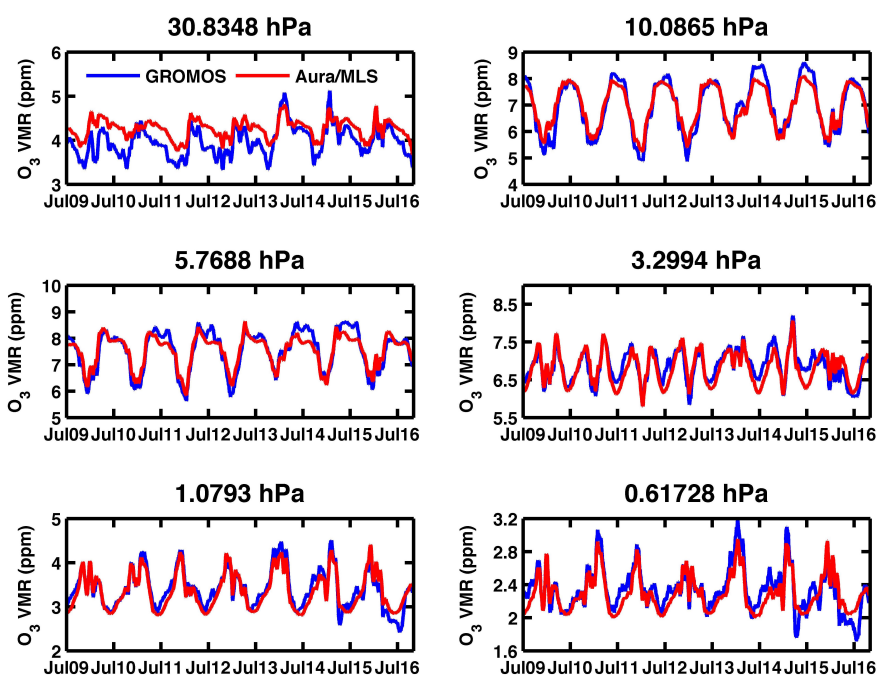
Figure 3. Time series of O_3 VMR measurements of GROMOS (blue line) and Aura/MLS (red line) for the period from July 2009 to November 2016 at different pressure levels. An averaging kernel smoothing has been applied to the series of the Aura/MLS measurements coincident in time and space with the GROMOS measurements. Both time series are smoothed in time by a moving average
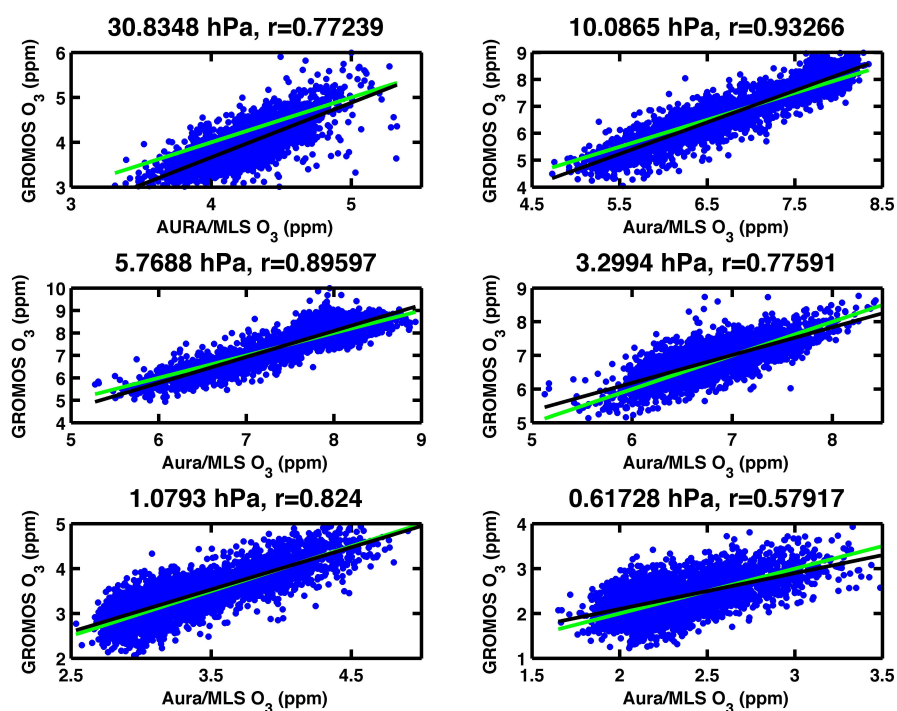
Figure 4. Scatter plots of coincident O_3 VMR measurements of GROMOS and Aura/MLS for the period from July 2009 to November 2016 at different pressure levels. The black line is the linear fit of both time series. The green line indicates the case of identity, O_3(Aura/MLS)=O_3(GROMOS). r values are correlation coefficients of the Aura/MLS and GROMOS time series
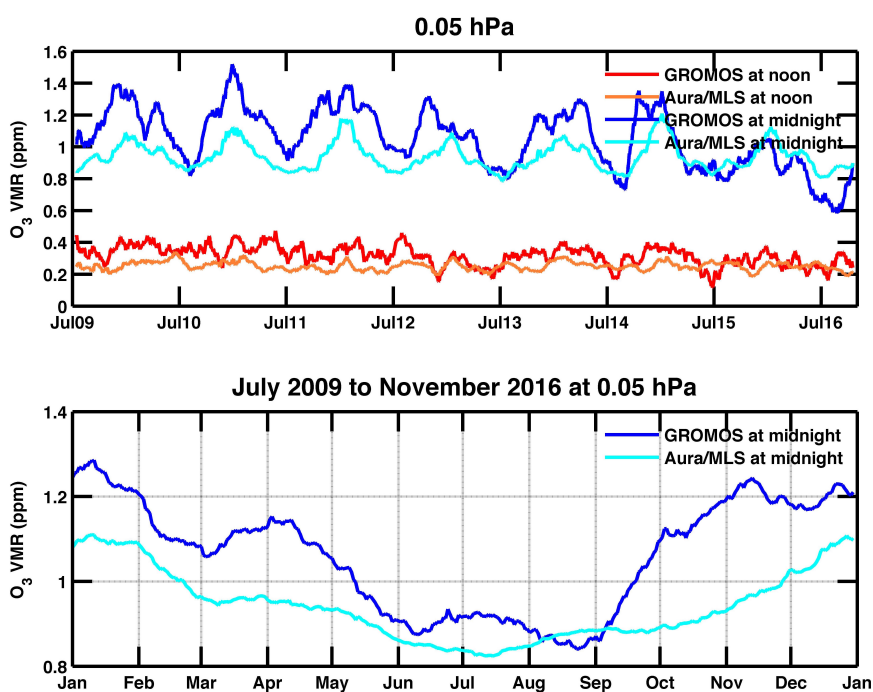
Figure 5. The first panel shows the diurnal variation of O_3 VMR measured at noon (GROMOS in red, Aura/MLS in orange) and at midnight (GROMOS in blue, Aura/MLS in cyan) at 0.05 hPa (70 km) ans the second panel shows its evolution throughout the year averaged for the time interval under assessment (July 2009–November 2016). All time series are smoothed in time by a moving average
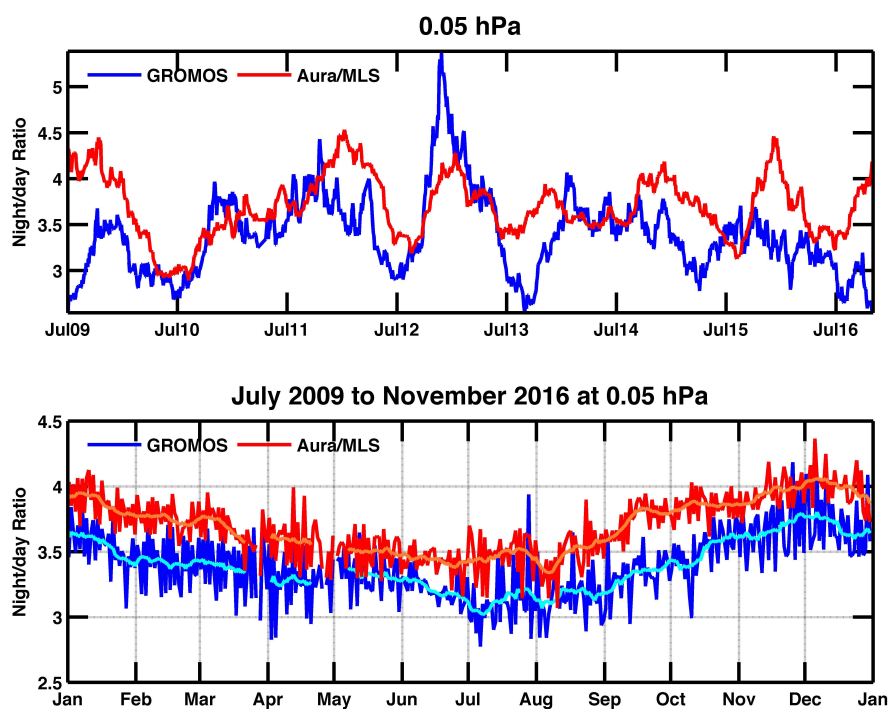
Figure 6. The first panel displays the night-to-day ratio (NDR) of GROMOS (blue line) and Aura/MLS (red line) at 0.05 hPa (70 km) for the time period from July 2009 to November 2016 and the second panel shows its evolution throughout the year averaged for this time period. All time series are smoothed in time by a moving average and the orange line (Aura/MLS) and the cyan line (GROMOS) shown in the second panel are averaged over 10 data points